An Investigation of Containerless Extrusion of Al-Zn-Mg Alloys

Geethalakshmi K.[1], A. O. Surendranathan[2]

[1]P. C. College of Engineering, Verna, Goa, [2]National Institute of Technology Karnataka, Surathkal

[1]geethashyam@gmail.com; [2] aos_nathan@rediffmail.com

Abstract

Extrusion is a complex process involving interaction between the process variables. A comprehensive investigation on containerless extrusion of Al-Zn-Mg alloys through open conical dies has been carried out to study the influence of extrusion strain, die included angle and zinc content on the quality of the extrusion and extrusion pressure. Billets of fixed cross-section were extruded through open dies of varying die included angle and land diameter. The limiting strain values and optimum die angles corresponding to the minimum extrusion pressure were calculated from the experimental data. It was observed that at 0.09 strain, pure extrusion is possible for all die angles from 12° to 30° in Al-5Zn-1Mg alloy and Al-10Zn-1Mg alloy whereas in Al-15Zn-1Mg alloys pure extrusion is possible only at lower die angles. For higher strain values, pure extrusion occurs over a narrow range of lower die angles.

Keywords:

Al-Zn-Mg Alloy; Containerless Extrusion; Optimum Die Angle; Limiting Strain

Introduction

Containerless extrusion is one of the types of extrusion. In this process, a billet is forward extruded without container or a large clearance between the container and the billet. Since extrusion is done without a container as against conventional extrusion, it is also called as open die extrusion, or free extrusion. Container wall-billet friction force is eliminated in containerless extrusion, which leads to a large reduction in the total force required for extrusion. Some important aspects of the open-die extrusion have been undertaken by Srinivasan and Venugopal [2004-2008], who have studied the containerless extrusion of *Ti-6Al-4V* and commercial purity titanium.

Fig. 1 represents the schematic illustration of containerless extrusion. The geometry of the operation is described by the semicone angle, the reduction ratio and the initial aspect ratio. The relevant material characteristics are the shear flow stress and the friction factor.

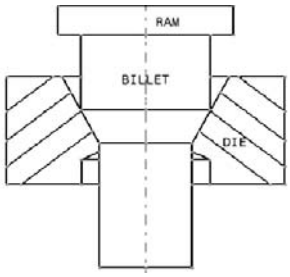

FIG. 1 CONTAINERLESS EXTRUSION

Even though aluminium alloys are considered to be excellent candidates for conventional extrusion, no researchhas been done to explore the possibility of containerless extrusion of aluiminium alloys. The high specific strength of Al-Zn-Mg alloys and the low processing force of containerless extrusion promises to be a vital combination, which needs to be further explored upon. Hence, in the present research work, the containerless extrusion of three compositions of Al-Zn-Mg alloy, i.e., Al-5Zn-1Mg, Al-10Zn-1Mg and Al-15Zn-1Mg are studied in detail by theoretical analysis using slab method [Avitzur, 1978], [Lange, 1985] and experimental analysis by conducting containerless extrusion experiments.

Theoretical Analysis

Deformation Work and Forces in Containerless Extrusion

The advantage of containerless extrusion is distinguished in the elimination of the friction component of the container and thus the forces during the extrusion process are ensured to be lowered. The total force consists of three terms only, i.e., ideal force, shear force and die friction force as the container wall billet friction is absent. The total force F_{Tot} can be calculated by the equation,

$$F_{Tot} = F_{Id} + F_{Fr} + F_{Sh} \quad (1)$$

where F_{Id} is the ideal force,
F_{Fr} is the die friction force,
and F_{Sh} is the shear deformation force

For a work hardening material, the ideal deformation work is given by,

$$W_{id} = V\sigma_{fm}\,\varepsilon \quad (2)$$

where V is the volume, σ_{fm} is the mean flow stress and

$$\varepsilon = \ln\left[\frac{Ao}{Af}\right]$$

The total frictional work along the die wall and in the deformation zone is

$$W_{FR} = V\sigma_{fm}\,\varepsilon\left[\frac{2\mu}{\sin 2\alpha}\right] \quad (3)$$

where 2α is the die included angle and μ is the friction coefficient

The total shearing work for the deformed volume will be

$$W_{Sh} = \frac{2}{3}V\sigma_{fm}\,\alpha \quad (4)$$

For the quasi-stationary portion of the extrusion process in the deformation zone,

$$\frac{W}{V} = \frac{F}{A_O} \quad (5)$$

Substituting the corresponding components of force, the total force for containerless extrusion may be written as ,

$$F_{Tot} = A_o\sigma_{fm}\left[\frac{3}{2}\alpha + (1+\frac{2\mu}{\sin 2\alpha})\varepsilon\right] \quad (6)$$

In other words, the expression for total punch pressure in containerless extrusion is given by,

$$P_P = \sigma_{fm}\left[\frac{3}{2}\alpha + (1+\frac{2\mu}{\sin 2\alpha})\varepsilon\right] \quad (7)$$

Eqn (7) illustrates that the deformation work and force are dependent on the die included angle 2α. The various components of forces for solid containerless extrusion can be plotted as a function of the die included angle 2α as shown schematically in Fig 2.

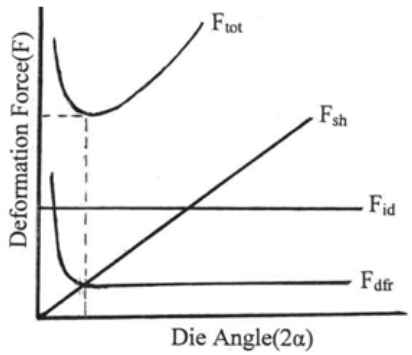

FIG. 2 SCHEMATIC VARIATION OF INDIVIDUAL FORCE COMPONENTS WITH THE DIE INCLUDED ANGLE

The angle at which the deformation force is a minimum is termed as the optimum die angle. Taking the derivative of Eqn. (6) with respect to α and equating it to zero, we can get the expression for the optimum die angle.

$$\cos 2\alpha_{opt} = -3\mu\varepsilon_{\max} \pm \sqrt{9\mu^2\varepsilon^2_{\max} + 1} \quad (8)$$

Experimental

Axisymmetric Compression and Ring Compression Tests

The flow properties of metals at large strains are most conveniently obtained by compressing a cylindrical specimen between a pair of parallel platens [Altan et. al., 1983]. Axisymmetric compression tests were carried out to determine the flow properties of the material and ring compression was used for determining the friction coefficient of the material - tests were performed at room temperature using a Universal Testing Machine with 40T capacity at a constant cross head speed of 3.3 x 10^{-3}m/sec. In order to get homogenous deormation, friction was minimized by lubricating bearing surfaces with graphite powder.

From the measured force–stroke data of axisymmetric compression test, the true stress-true strain curves were plotted. According to the flow equation, a log–log plot of true stress and true strain will result in a straight line. The linear slope of this line is the strain hardening exponent (*n*) and the strength coefficient (K) is the true stress at ε = 1.

From ring compression test, reduction in height and increase in internal diameter of the ring test specimens were measured. Using the Male and Cockroft calibration chart, the friction factors were calculated.

The average flow properties and the friction coefficients of the three alloy compositions are presented in Table 1.

TABLE 1 AVERAGE FLOW PROPERTIES AND FRICTION COEFFICIENT OF THREE ALLOY COMPOSITIONS

Alloy Composition	Strength Coefficient (MPa)	Strain Hardening Exponent	Friction Coefficient
Al-5Zn-1Mg	308.99	0.0856	0.49
Al-10Zn-1Mg	347.83	0.0973	0.4
Al-15Zn-1Mg	383.75	0.178	0.25

Containerless Extrusion Tests

1) Preparation of Test Specimens

Commercial pure aluminium, zinc and magnesium were weighed in the required proportion. First,

aluminum was melted until it is in the liquid condition. After complete melting of aluminum, the required amount of zinc was added to the melt. Magnesium addition was made just before pouring. To avoid burning at the surface of the melt, magnesium was packed inside pure aluminum foil and this package was directly added into the melt, and a little stirring was carried out. The dross was skimmed off manually and the melt was poured into cylindrical moulds. The ingots were homogenized at 400°C for 8 hr in a muffle furnace. The chemical compositions of the three alloys are presented in Table 2.

TABLE 2 CHEMICAL COMPOSITION OF THE THREE ALLOYS

Element	Chemical Composition (wt%)		
	Alloy 1	Alloy 2	Alloy 3
Si	0.86	0.69	0.74
Fe	0.24	0.19	0.23
Cu	0.02	0.01	0.01
Mn	0.56	0.53	0.5
Mg	1.26	1.13	1.22
Cr	0.01	0.01	0.01
Zn	5.12	10.1	14.4
Al	Balance	Balance	Balance

2) *Design and Making of Dies*

In order to carry out the containerless extrusion experiment, conical dies of included angles 12°, 15°, 25°, 30° and 40° with land diameter corresponding to strains of 0.09, 0.13, 0.18, 0.21and 0.28 were made from high carbon high chromium steel, hardened and tempered to HRC 50. The design of a typical die is shown in Fig.3.

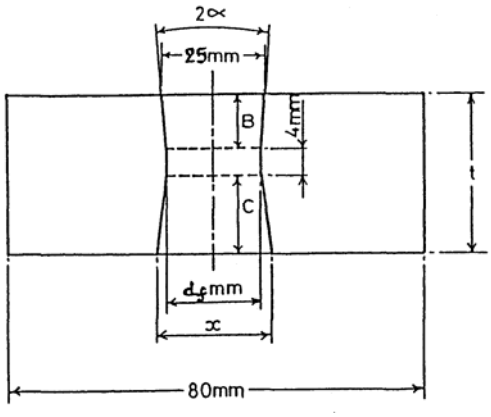

FIG.3 DESIGN OF A TYPICAL CONICAL DIE

3）*Extrusion Experiments*

Billets with 25mm diameter and height to diameter ratio of 1.5 were machined from the homogenised alloys and annealed at 400°C. The internal walls of the conical die and the outer wall of the billets were carefully lubricated with powdered graphite mixed with engine oil and extruded through the dies at room temperature. The velocity of the ram was maintained at 3 x 10^{-3}m/s. For each test, the force stroke data were recorded and plotted. Tests were repeated on dies corresponding to different combinations of die angles and land diameters. The maximum extrusion load for each extrusion test were determined and recorded. The extrusion pressure was calculated from the maximum extrusion load divided by the original cross-sectional area of the test specimen.

Results and Discussion

Theoretical Punch Pressure Variation

The strength coefficient and the stain hardening exponent values obtained from the compression and ring compression tests were used to determine the flow stress values of the three alloy compositions. The theoretical punch pressure was calculated for different die included angles and extrusion strains using slab method. The variation of theoretical punch pressure with die angle is shown in Fig 4(a) and the variation of theoretical punch pressure with the extrusion strain is shown in Fig.4(b).

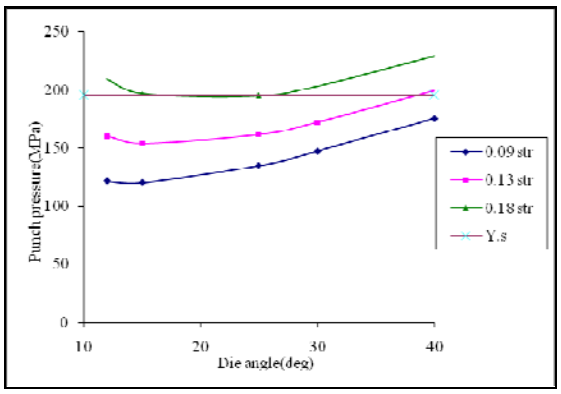

(a)

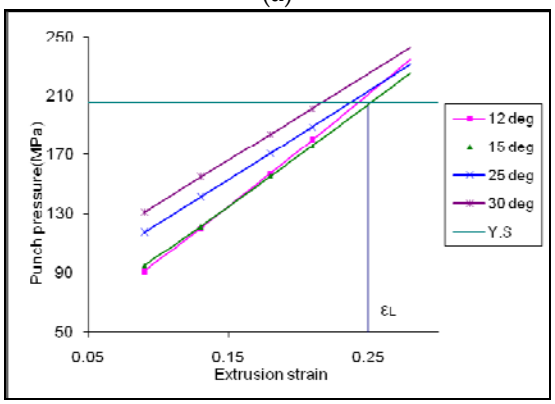

(b)

FIG. 4 VARIATION OF THEORETICAL PUNCH PRESSURE WITH (A) DIE ANGLE AND (B) EXTRUSION STRAIN

Extrusion Force Stroke Diagrams

A typical force-stroke diagram for extrusion through the conical die at a particular extrusion strain is presented in Fig. 5.

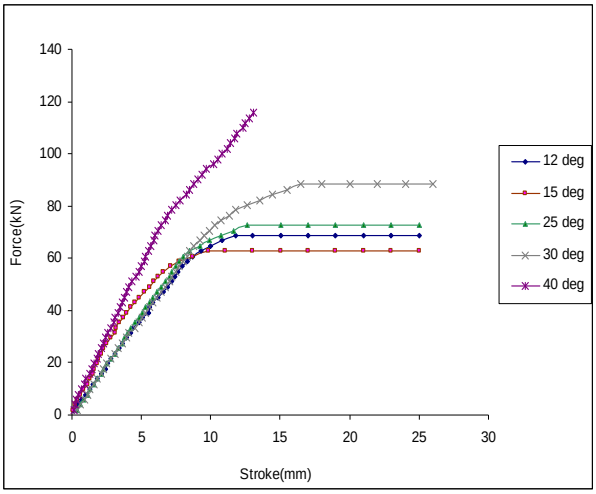

FIG. 5 A TYPICAL FORCE – STROKE DIAGRAM

The force stroke diagram indicates two regions namely the region of increasing force due to initial die filling and thereafter the region of constant force if extrusion has taken place. The maximum punch force which occurs after a certain punch penetration, indicates the initial reduction of the work material to fill the zone between the die entry and exit planes and it corresponds to the minimum pressure required to initiate the extrusion process. As the billet extrudes through the die, the pressure required to maintain the flow progressively declines with decreasing length of the billet and can be observed that at certain combinations of strain and die angle, force remains constant after the initial rise, otherwise it increases continuously with increasing movement of ram with a slope change. The change in slope distinguishes between the initial die filling and upsetting regions where as the constant force indicates pure extrusion.

For a given die angle and work piece material, when the flow stress (σ_{fm}) and friction coefficient are constant, the punch pressure varies directly as the extrusion strain. Therefore for any given die angle, a strain exists, above which the pure extrusion is not possible. Upsetting of the billet above the die entrance starts and this occurs when the punch pressure value reaches the yield stress value of the work piece material. When the punch pressure for extrusion equals the yield stress for a particular extrusion strain, that strain is called the limit strain (ε_L). At extrusion strains of 0.09 and 0.13, pure extrusion occurs for all die included angles from 12° to 40°. However, at 0.18 strain, upsetting is found to dominate over pure extrusion for die included angle of 40° as indicated by the continuous increase of force with ram displacement. With further increase in extrusion strain, the range of die angle favourable for pure extrusion narrows down to lower values around 15°.

Dependence of Punch Pressure on Die Included Angle

If sliding distance between the billet and die is large, friction will be more. Friction decreases with increase in die angle because of the decrease in sliding length. With a too large cone angle, the redundant work due to inhomogeneous deformation becomes a dominant factor and distortion predominates over pure extrusion. In other words, sound flow occurs only within a limited domain. In order to find the dependence of punch pressure on die included angle, punch pressure is plotted as a function of die angle, under constant reduction, friction and flow stress. For a given extrusion strain, point of minimum stress indicates on the abscissa the value of the optimal die angle. Fig. 6 represents the dependence of punch pressure on the die included angle.

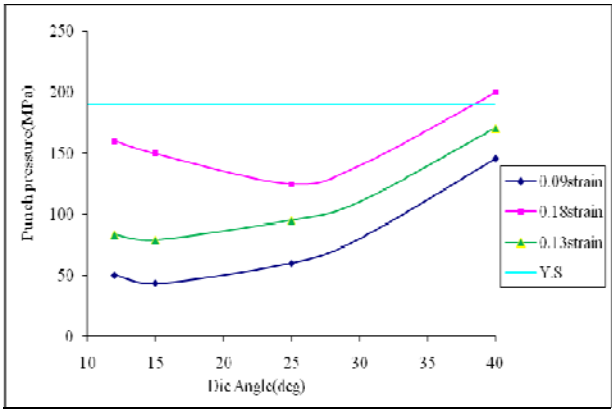

FIG. 6 VARIATION OF EXPERIMANTAL PUNCH PRESSURE WITH DIE ANGLE

Observation of Fig. 6 reveals that for 0.09 and 0.13 extrusion strains, the punch pressure decreases with increase in die included angle up to 15-20° and then increases while for 0.18 strains, it decreases with die angle up to 25° and thereafter, it increases with increase in die angle. For extrusion strains of 0.09 and 0.13, it can be seen that there is possibility for pure extrusion even beyond 40° die angle and around 25°die angle, there is still scope for pure extrusion above 0.18 strain. However, it is very clear that increment in either the die angle or the extrusion strain brings about an increase in the minimum punch pressure value. This die angle for which the punch pressure is minimum is called the optimum die angle

for that strain. This is due to that fact that, with too small a cone angle, the length of contact between the billet and the die is large, causing significantly high frictional losses. The optimum die angles of the three alloys at different strains are presented in Table 3

TABLE 3 OPTIMUM DIE ANGLES OF THE THREE ALLOYS AT DIFFERENT EXTRUSION STRAINS

Alloy	Extrusion strain	Optimum die angle
Al-5Zn-1Mg	0.09	15
	0.13	20
	0.18	25
Al-10Zn-1Mg	0.09	25
	0.13	27
	0.18	30
Al-15Zn-1Mg	0.09	25
	0.13	25

Dependence of Punch Pressure on Extrusion Strain

Fig. 7 represents the dependence of Experimental punch pressure on the extrusion strain.

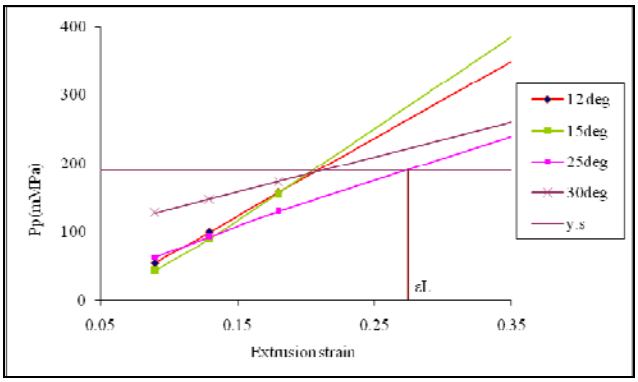

FIG. 7 VARIATION OF EXPERIMENTAL PUNCH PRESSURE WITH EXTRUSION STRAIN

Fig. 7 shows that punch pressure varies linearly with the extrusion strain. Extrapolating each plot of extrusion strain vs punch pressure to intercept the experimental flow stress values gives the limiting strain for each die angle. The limiting strain, at which damages to the structure of material occur, depends on the combination of stress components acting in the critical zone of the formed piece. When the actual punch pressure reaches the flow stress value, the limit for pure extrusion through the die cavity ceases and the tendency for lateral deformation becomes more probable than pure extrusion.

Inflence of Alloy Composition

The SEM micrographs of the three alloy compositions in the annealed condition are presented in Fig. 8.

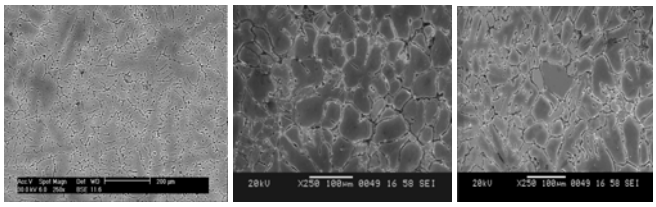

a) (b) (c)

FIG. 8 SEM MICROGRAPHS OF (A) AL-5ZN-1MG, (B) AL-10ZN-1MG AND (B) AL-15ZN-1MG ALLOY

It was observed that as the Zn content increases, the punch pressure tends to increase as well. This can be attributed to the fact that an increase in the zinc concentration leads to more dispersed precipitation with formation of a narrow zone, free of precipitation in the grain boundaries which promote strain localization in the grain boundary vicinity [Gerchikova et. al, 1972], [Dumont et. al, 2003]. In addition, according to the data on the phase equilibrium in the Al-Zn alloys, the solubility of Zn and Mg in aluminium does not exceed 1% at room temperature [Massalski, 1993]. In other words, the aluminium solid solution is in a supersaturated state. Previous works on aluminium alloy [Mazilkin et. al, 2007] have shown that the grains in the alloys become significantly smaller due to deformation and the hardness of the alloy increases slightly with the Mg and Zn concentrations.

The comparison of limiting strain values from experimental analysis and theoretical analysis for Al-5Zn-1Mg, Al-10Zn-1Mg and Al-15Zn-1Mg alloys are presented in Table 4.

TABLE 4. COMPARISON OF LIMITING STRAIN VALUES

Alloy	Limiting strain	
	Experimental	Theoretical
Al-5Zn-1Mg	0.28	0.25
Al-10Zn-1Mg	0.18	0.16
Al-15Zn-1Mg	0.15	0.15

The results of the experimental and theoretical analysis show the same trend. However, the punch pressure values obtained in the theoretical analysis is found to be on the higher side as compared to experimental ones. Also, it can be seen from Table 4 that, the limiting strain value is higher in experimental results than that in theoretical analysis. This is due to the reduced flow stress values of the material during deformation resulting from temperature rise in the deformation zone as a consequence of adiabatic and frictional heating. These two temperature aspects transform the isothermal transformation into an in-situ warm extrusion which is responsible for the lower values of the experimental punch pressure.

Conclusion

As the extrusion strain increases, upsetting dominates over pure extrusion. Punch pressure value increases with the increment in Zn content. For extrusion strain of 0.09, pure extrusion is possible for all die angles from 12° to 30° in Al-5Zn-1Mg alloy and Al-10Zn-1Mg alloy whereas in Al-15Zn-1Mg alloys pure extrusion is possible only at lower die angles. For higher strain values, pure extrusion occurs over a narrow range of lower die angles.

Results of theoretical and experimental analysis are comparable and in good agreement with one another. Limit strain values obtained are higher in the experimental analysis as compared to theoretical analysis. The increase in temperature due to adiabatic and friction heating at the deformation zone reduces the resistance to deformation and facilitates a higher reduction.

REFERENCES

Altan T., Oh S. and Gegel H.L., "Metal Forming: Fundamentals and Applications", American Society for Metals, USA, 1983, 48-53.

Avitzur B., "Metal Forming: Processes and Analysis", Tata McGraw Hill, New Delhi, 1978, 225-230.

Dumont D., Deschamps, A. and Brechet, Y., "On the Relationship Between Microstructure, Strength and Toughness in AA7050 Aluminium Alloy", Mat. Sci. and Eng. A356, 2003, 326-336.

Gerchikova N.S., Fridlyander I.N., Zaitseva N.I. and Kirkina N.N., "Change in the Structure and Properties of Al-Zn-Mg Alloys", Metall. Itermich. Obrab. Metall., 3, 1972, 47-50.

Lange K., "Fundamentals of Metal Forming", McGraw Hill Book Company, 1985, 13.1-13.20.

Massalski T.B., "Binary Alloy Phase Diagrams", ASM International, Materials Park, Ohio, 1993, 2.30-2.56.

Mazilkin A.A., Straumal B.B., Protasova S.G., Kogtenkova O.A. and Valiev R.Z., "Structural Changes in Aluminium Alloys Upon Severe Plastic Deformation", Physics of Solid State, 49-5, 2007, 868-873.

Srinivasan, K. and Venugopal, P., "Direct and Inverted Open Die Extrusion of Rods and Tubes", J. Mater. Process.Technol., 153-154, 2004, 765-770.

Srinivasan, K. and Venugopal, P., "Influence of Die Angle on the Open Die Extrusion of Commercially Pure Titanium Tubes", Material and Manufacturing Processes, 22, 2007, 238-242.

Srinivasan, K. and Venugopal, P., "Formability Limit in Containerless (open die) Extrusion of Commercial Purity Titanium Rods and Tubes", Material and Manufacturing Processes, 23, 2008, 347-351.

.